

Supplementary Information

Rational synthesis of chiral layered magnets by functionalization of metal simple hydroxides with chiral and non-chiral Ni(II) Schiff base complexes

Émilie Delahaye, Séraphin Eyele-Mezui, Mayoro Diop, Cédric Leuvrey, Pierre Rabu and Guillaume Rogez

Experimental details

General remarks

The synthesis of **Ni(SalenSO₃)Na₂**, **Ni((R,R)CySalenSO₃)NaK**, and **Ni((S,S)CySalenSO₃)NaK** was performed according to published procedures.¹

Cu₂(OH)₃(DS)² and Co₂(OH)₃(DS₀)³ were prepared as previously described. All experiments were conducted under argon, and the solvents were degassed prior to use. Yields of the synthesis of hybrid compounds are around 50-70%.

Elemental analyses for C, H, N, S, Co, and Cu were carried out at the Service Central d'Analyse of the CNRS (USR-59). The powder XRD patterns were collected with a Bruker D8 diffractometer (Cu K α_1 = 1.540598 Å) equipped with a SolX detector discriminating in energy. ¹H NMR spectra were recorded on a Bruker AVANCE 300 (300 MHz) spectrometer. The internal references of the spectrum correspond to the peak of the non deuterated solvent. The SEM images were obtained with a JEOL 6700F (scanning electron microscope (SEM) equipped with a field emission gun, operating at 3 kV in the SEI mode) instrument. FT-IR spectra were collected on a Digilab FTS 3000 computer-driven instrument (0.1 mm thick powder samples in KBr). UV/Vis/NIR studies were performed on a Perkin-Elmer Lambda 950 spectrometer (spectra recorded in the reflection mode, using a 150 mm integrating sphere, with a mean resolution of 2 nm and a sampling rate of 300 nm·min⁻¹). Circular dichroism was measured on a Jasco 810 spectrometer, in the solid state, using 0.1 mm thick powder samples in KBr. TGA-TDA experiments were performed using a Setaram TG92 instrument (heating rates of 5°C·min⁻¹, air stream). The magnetic studies were carried out with a SQUID

magnetometer (Quantum Design MPMS-XL) covering the temperature and fields ranges 2-300 K, ± 5 T. ac susceptibility measurements were performed in a 0.35 mT alternative field (100 Hz). Magnetization measurements at different fields at room temperature confirm the absence of ferromagnetic impurities.

- Synthesis of the hybrid compounds.

Ni(SalenSO₃)₂Cu (1) : Ni(SalenSO₃)Na₂ (528 mg, 0.91 mmol) was dissolved in 160 mL of a 1/1 v:v water-ethanol mixture. At this stage, Cu₂(OH)₃(DS) (260 mg, 0.59 mmol) was added and the mixture was stirred for 1.5 h at 70° C under argon. The orange-brown powder was filtered and washed with water and ethanol. R = 60-70 %.

Anal. for Cu₂(OH)_{3.24}(Ni(SalenSO₃))_{0.38}·2.6 H₂O : Cu₂Ni_{0.38}C_{6.08}H_{7.8}N_{0.76}S_{0.76}O_{6.28}·2.6 H₂O (*M* = 412.1 g / mol) Found (Calc.) (%) : Cu, 31.18 (30.84); Ni, 5.90 (5.41); C, 17.83 (17.70); H, 2.93 (3.16); N, 2.21 (2.58); S, 6.38 (5.91). IR (KBr pellet, cm⁻¹) : 3453 s, 2924 w, 2855 w, 1624 s, 1535 m, 1467 m, 1429 w, 1383 m, 1318 m, 1201 s, 1168 s, 1113 s, 1031 s, 832 w, 739 w, 679 w, 635 w, 606 m, 508 w, 469 w, 426 w.

Ni(SalenSO₃)₂Co (2) : Ni(SalenSO₃)Na₂ (528 mg, 0.91 mmol) was dissolved in 160 mL of a 1/1 v:v water-ethanol mixture. At this stage, Co₂(OH)₃(DS₀) (260 mg, 0.62 mmol) was added and the mixture was stirred for 4 hours at 85° C under argon. The orange-brown powder was filtered and washed with water and ethanol. R = 60-70 %.

Anal. for Co₂(OH)_{3.18}(NiSalenSO₃)_{0.41}·4 H₂O : Co₂Ni_{0.41}C_{6.56}H_{8.1}N_{0.82}S_{0.82}O_{6.46}·4 H₂O (*M* = 442.1 g / mol) Found (Calc.) (%) : Co, 26.50 (26.66); Ni, 5.90 (5.44); C, 18.08 (17.82); H, 4.13 (3.67); N, 2.19 (2.59); S, 4.50 (5.94). IR (KBr pellet, cm⁻¹) : 3446 s, 2974 w, 1633 s, 1603 s, 1538 m, 1469 s, 1433 w, 1383 s, 1311 w, 1219 s, 1200 s, 1171 s, 1114 s, 1032 s, 954 w, 829 w, 738 w, 678 w, 636 m, 607 m, 558 w, 528 w, 462 w.

Ni((R,R)CySalenSO₃)₂Cu (3) : Ni((R,R)CySalenSO₃)NaK (300 mg, 0.46 mmol) was dissolved in 50 mL of a 1/1 v:v water-ethanol mixture. At this stage, Cu₂(OH)₃(DS) (130 mg, 0.29 mmol) was added and the mixture was stirred for 3 hours at 90° C under argon. The orange-brown powder was filtered and washed with water and ethanol. R = 50-60 %.

Anal. for Cu₂(OH)_{3.20}(Ni(R,R)CySalenSO₃)_{0.40}·2.8 H₂O : Cu₂Ni_{0.4}C₈H_{10.4}N_{0.8}S_{0.8}O_{6.4}·2.8 H₂O (*M* = 446.8 g/mol) Found (Calc.) (%) : Cu, 28.63 (28.44); Ni, 4.87 (5.25); C, 21.96 (21.50); H, 3.51 (3.61); N, 2.15 (2.51); S, 5.44 (5.74). IR (KBr pellet, cm⁻¹): 3443 s, 2924 w, 2856 w, 1619 s, 1559 w, 1537 m, 1470 m, 1422 w, 1383 w, 1345 w, 1320 w, 1197 s, 1168 s, 1111 s, 1030 s, 959 w, 932 w, 833 w, 752 w, 688 w, 621 m, 579 w, 523 w, 444 w.

Ni((S,S)CySalenSO₃)₂Co (4) : Ni((S,S)CySalenSO₃)NaK (300 mg, 0.46 mmol) was dissolved in 50 mL of a 1/1 v:v water-ethanol mixture. At this stage, Cu₂(OH)₃(DS) (130 mg, 0.29 mmol) was added and the mixture was stirred for 3 hours at 90° C under argon. The orange-brown powder was filtered and washed with water and ethanol. R = 50-60 %.

Anal. for Cu₂(OH)_{3.22}((S,S)NiCySalenSO₃)_{0.39}·2.8 H₂O : Cu₂Ni_{0.39}C_{7.8}H_{10.24}N_{0.78}S_{0.78}O_{6.34}·2.8 H₂O (*M* = 441.8 g/mol) Found (Calc.) (%) : Cu, 29.57 (28.77); Ni, 4.68 (5.18); C, 22.03 (21.21); H, 3.72 (3.61); N, 2.24 (2.47); S, 4.73 (5.66). IR (KBr pellet, cm⁻¹): 3445 s, 2935 w, 2860 w, 1621 s, 1558 w, 1537 m, 1469 m, 1423 w, 1384 w, 1346 w, 1320 w, 1198 s, 1167 s, 1111 s, 1031 s, 964 w, 932 w, 833 w, 754 w, 689 w, 622 m, 579 w, 511 w, 446 w.

Ni((R,R)CySalenSO₃)₂Co (5) : Ni((R,R)CySalenSO₃)NaK (300 mg, 0.46 mmol) was dissolved in 50 mL of a 1/1 v:v water-ethanol mixture. At this stage, Co₂(OH)₃(DS₀) (130 mg, 0.31 mmol) was added and the mixture was stirred for 6 hours at 90° C under argon. The dark-green powder was filtered and washed with water and ethanol. R = 50-60 %.

Anal. for Co₂(OH)_{3.40}((R,R)NiCySalenSO₃)_{0.30}·3.5 H₂O : Co₂Ni_{0.3}C₆H_{8.8}N_{0.6}S_{0.6}O_{5.8}·3.5 H₂O (*M* = 399.9 g/mol) Found (Calc.) (%) : Co, 29.45 (29.47); Ni, 4.95 (4.40); C, 18.18 (18.02); H, 3.90 (3.98); N, 1.85 (2.10); S, 3.35 (4.81). IR (KBr pellet, cm⁻¹): 3454 s, 2922 w, 2853 w, 1622 s, 1601 m, 1537 m, 1469 m, 1425 w, 1383 w, 1346 w, 1324 w, 1199 s, 1171 s, 1112 s, 1032 s, 962 w, 933 w, 833 w, 751 w, 689 w, 621 m, 579 w, 553 w, 525 w, 449 w.

Ni((S,S)CySalenSO₃)₂Co (6) : Ni((S,S)CySalenSO₃)NaK (300 mg, 0.46 mmol) was dissolved in 50 mL of a 1/1 v:v water-ethanol mixture. At this stage, Co₂(OH)₃(DS₀) (130 mg, 0.31 mmol) was added and the mixture was stirred for 6 hours at 90° C under argon. The dark-green powder was filtered and washed with water and ethanol. R = 50-60 %.

Anal. for Co₂(OH)_{3.36}((S,S)NiCySalenSO₃)_{0.32}·3.1 H₂O : Co₂Ni_{0.32}C_{6.4}H_{9.08}N_{0.64}S_{0.64}O_{5.88}·3.1 H₂O (*M* = 402.1 g/mol) Found (Calc.) (%) : Co, 29.71 (29.31); Ni, 4.16 (4.67); C, 19.36 (19.12); H, 4.05 (3.77); N, 1.91 (2.23); S, 3.35 (5.10). IR (KBr pellet, cm⁻¹): 3457 s, 2921 w, 2852 w, 1623 s, 1602 m, 1536 m, 1469 m, 1425 w, 1383 w, 1346 w, 1324 w, 1199 s, 1169 s, 1112 s, 1032 s, 964 w, 934 w, 833 w, 749 w, 689 w, 621 m, 579 w, 554 w, 529 w, 448 w.

TGA-TDA

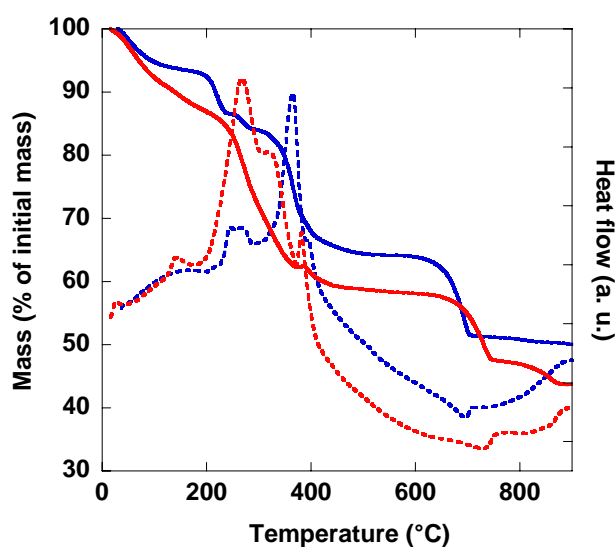


Fig. S1 TGA (full lines) and TDA (dotted lines) curves for Ni(SalenSO₃)₂Cu (**1**) (blue) and Ni(SalenSO₃)₂Co (**2**) (red).

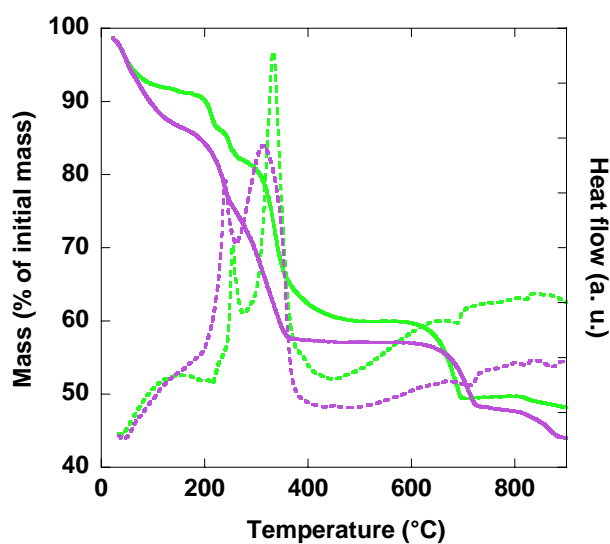


Fig. S2 TGA (full lines) and TDA (dotted lines) curves for Ni((R,R)CySalenSO₃)₂Cu (**3**) (green) and Ni((R,R)CySalenSO₃)₂Co (**5**) (purple).

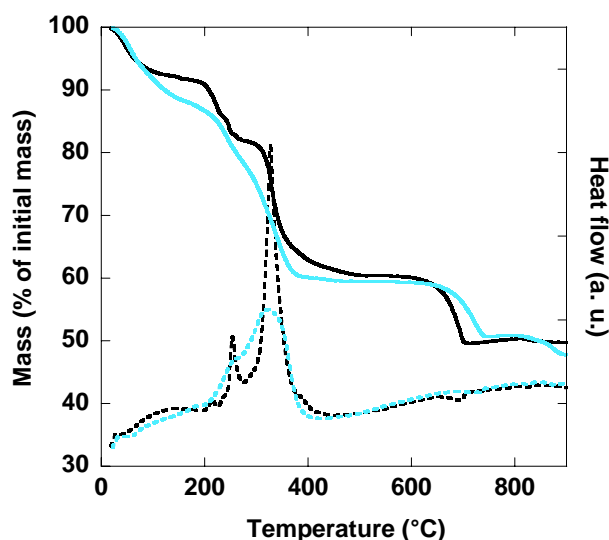


Fig. S3 TGA (full lines) and TDA (dotted lines) curves for $\text{Ni}((\text{S,S})\text{CySalenSO}_3)_2\text{Cu}$ (**4**) (black) and $\text{Ni}((\text{S,S})\text{CySalenSO}_3)_2\text{Co}$ (**6**) (cyan).

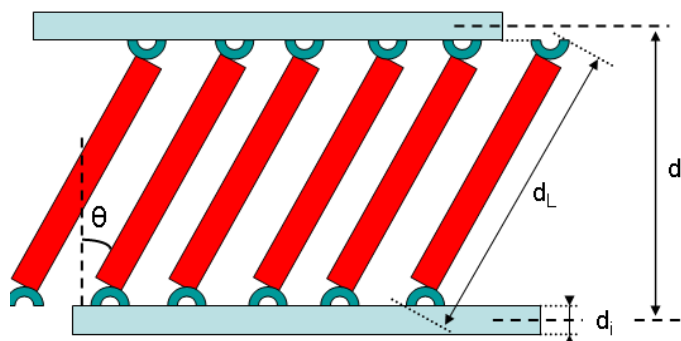
The TGA/TDA, represented on Fig. S1, S2, and S3 were obtained in air with a heating rate of $5^\circ\text{C}\cdot\text{min}^{-1}$. TGA of the cobalt and copper hydroxide-based compounds are rather similar and indicate a multi-step decomposition. The first event, between 20°C and 200°C , is slightly endothermic and corresponds to the loss of adsorbed and/or hydrogen-bonded interlayer water molecules. The quantities of water measured by TGA experiments are consistent with the stoichiometric formulae determined by elemental analysis (**1** : 7.3% (11.3% from elemental analysis), **2** : 13.9% (16.3%), **3** : 8.9% (11.4%), **4** : 8.5% (11.4%), **5** : 14.0% (15.8%), **6** : 12.0% (13.9%)).

A second region, between *ca.* 200°C and *ca.* 500°C corresponds to a series of poorly resolved exothermic events associated with both to the decomposition of the organic part of the intercalated complex and to the dehydroxylation of the inorganic layers.⁴⁻⁷ The last step around 750°C for **1** and 800°C for **2** can be ascribed to complete oxidative elimination of the residues derived from the pyrolysis of the initial sulfonate groups.^{8,9}

The final thermal decomposition products correspond to the formation of mixed oxides Cu/Ni or Co/Ni for copper compounds and cobalt compounds respectively, whose compositions, measured by EDX analysis, correspond to the ones inferred by elemental analysis.

Structural characterisation

Considering the following scheme :



Scheme S1 structural model of the lamellar hybrids

$d_L = 1.51$ nm for both **Ni(SalenSO₃)** and **Ni(CySalenSO₃)**, from single crystal structure.¹

For the copper hydroxide based compounds, an estimation of the inorganic layer thickness can be obtained from the structure of Gerhardtite $\text{Cu}_2(\text{OH})_3\text{NO}_3$ $d_i = 0.3$ nm.^{10, 11}

For the cobalt hydroxide based compounds, an estimation of the inorganic layer thickness can be obtained from the structure of $\text{Zn}_5(\text{OH})_6(\text{CO}_3)_2$ $d_i = 0.73$ nm.¹²

We therefore obtain for **1** ($d = 1.76$ nm) $\theta = 15^\circ$, for **2** ($d = 2.22$ nm) $\theta = 9^\circ$, for **5(6)** ($d = 2.20$ nm) $\theta = 13^\circ$.

For **3 (4)**, d_L is slightly larger (by 0.1 nm) than $(d-d_i)$. This can be due to the approximations made, or to the fact that the sulfonate-metal bonds can be a little bit longer than for the other ligands. In any case, it means that the **Ni(CySalenSO₃)** can be considered as perpendicular to the inorganic layers.

Scanning Electron Microscopy (SEM)

The SEM photos of compounds **Ni((S,S)CySalenSO₃)₂Cu (4)** and **Ni((S,S)CySalenSO₃)₂Co (6)** are shown on Figure S4 and are representative of all the compounds. These images are typical of this class of hybrid materials, which are obtained as thin platelet shaped microcrystals, in agreement with the lamellar character of their structure. The morphology and the size of the crystallites of the hybrid materials are very similar to the ones of the starting materials, consistently with what is observed by X-ray diffraction. In addition, the composition analysis by EDX (cartography of a $10^4 \mu\text{m}^2$ area along with several $1 \mu\text{m}^2$ spot analyses) underlines the homogeneity of the different compounds.

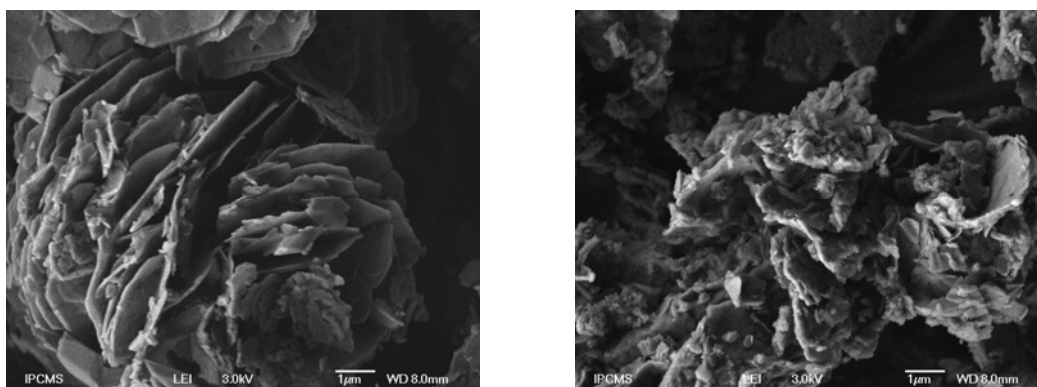


Fig. S4 SEM images of compounds $\text{Ni}((\text{S,S})\text{CySalenSO}_3)\text{Cu}$ (**4**) (left) and $\text{Ni}((\text{S,S})\text{CySalenSO}_3)\text{Co}$ (**6**) (right).

Infrared spectroscopy

The structure of the compounds was also investigated by FT-IR spectroscopy. The spectra show a broad band in the hydroxyl stretching region ($3600\text{--}3000\text{ cm}^{-1}$) which corresponds to the lattice water,¹³ in accordance with the chemical analysis. The vibrations bands in the 2900 cm^{-1} region, characteristic of the CH_2 elongation, are rather weak compared to the spectra of the starting materials (Figure S7). This is a good indication that there is no remaining dodecylsulfate or dodecylsulfonate in the hybrid compounds **1-6**. The absorption bands coming from the $[\text{Ni}(\text{SalenSO}_3)]^{2-}$ or the $[\text{Ni}((\text{R,R})\text{CySalenSO}_3)]^{2-}$ complexes appear between 1600 cm^{-1} and 400 cm^{-1} . Figures S5 and S6 underline the similarities between the spectra of the hybrid compounds and the ones of the starting complex in this region. Yet small variations occur. In particular, the absorption bands of the imine group around 1630 cm^{-1} and the absorption band of the C-O bond around $1260\text{--}1180\text{ cm}^{-1}$ are slightly shifted with respect to the starting complex. This may be due to the influence of the inorganic host on the rigidity of the complex. Finally, the identification of the asymmetric and symmetric vibrations of the sulfonate groups is of particular importance in order to precise the coordination mode of the ligands.^{9, 11, 14, 15} The stretching of the sulfonate moieties occurs around $1230\text{--}1120\text{ cm}^{-1}$ for the antisymmetrical mode (ν_{as}) and around $1080\text{--}1025\text{ cm}^{-1}$ for the symmetrical mode (ν_{s}). The difference $\Delta\nu$ between ν_{as} and ν_{s} , brings information on the mode of coordination of the sulfonate. In the present case, $\Delta\nu$ for the hybrid compounds is around $135/140\text{ cm}^{-1}$ (137 cm^{-1} for **1**, 139 cm^{-1} for **2**, 137 cm^{-1} for **3**, and 138 cm^{-1} for **5**) which suggests a monodentate mode of coordination for the sulfonate groups, with in addition probably one oxygen atom involved in a hydrogen bond.^{1, 9, 11, 14, 15}

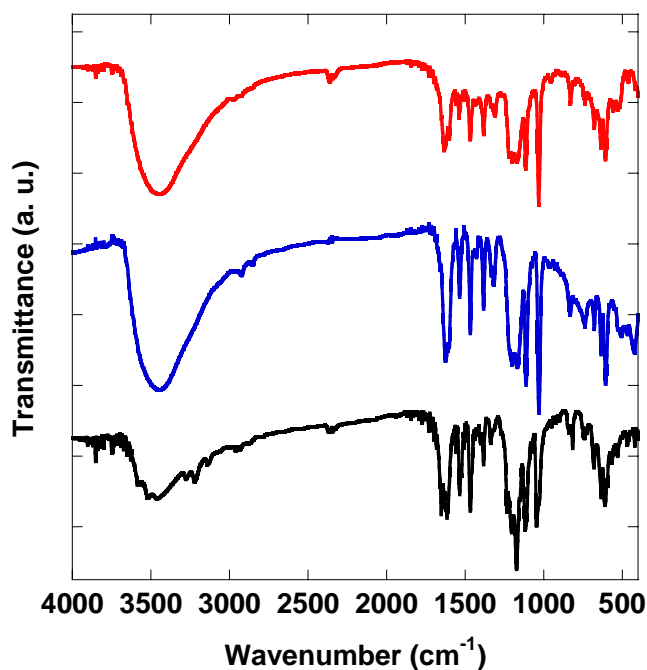


Fig. S5 Infrared spectra of the hybrid compounds Ni(SalenSO₃)Cu (1) (blue) and Ni(SalenSO₃)Co (2) (red), compared to the starting Ni(SalenSO₃)Na₂ complex (black).

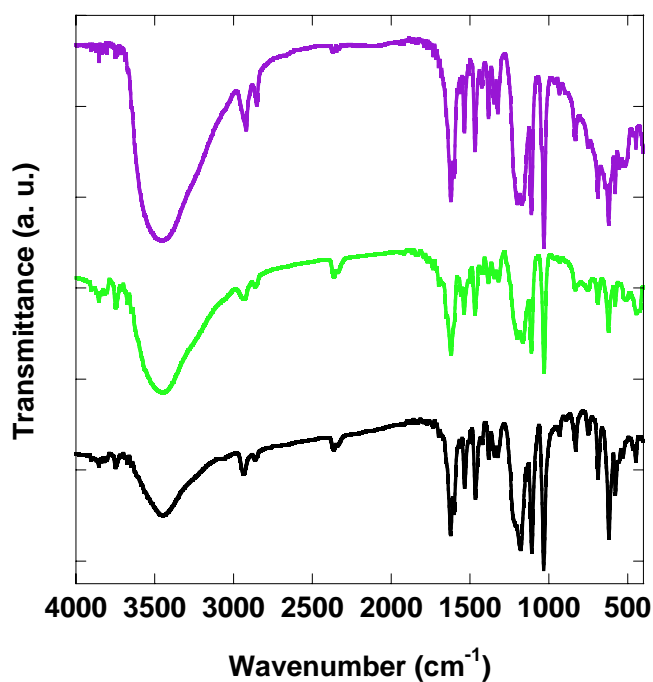


Fig. S6 Infrared spectra of the hybrid compounds Ni((R,R)CySalenSO₃)Cu (3) (green) and Ni((R,R)CySalenSO₃)Co (5) (purple), compared to the starting Ni((R,R)CySalenSO₃) complex (black).

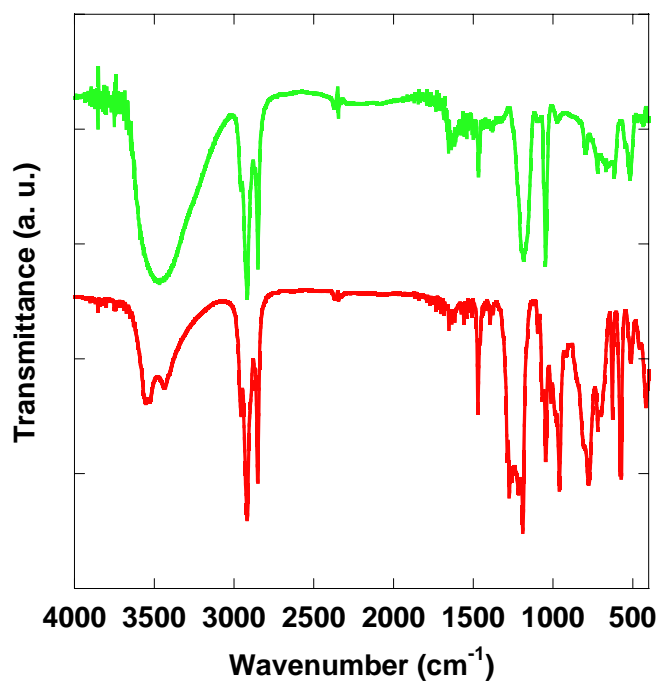


Fig. S7 Infrared spectra of the starting compounds $\text{Cu}_2(\text{OH})_3(\text{DS})$ (red) and $\text{Co}_2(\text{OH})_3(\text{DS}_0)$ (green).

Magnetic properties

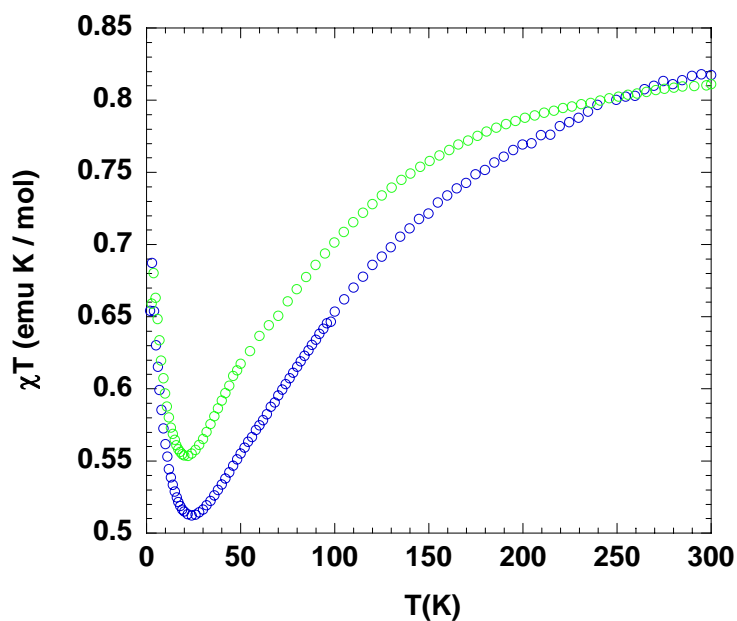


Fig. S8 $\chi T = f(T)$ for $\text{Ni}(\text{SalenSO}_3)_2\text{Cu}$ (1) (blue) and $\text{Ni}((\text{R,R})\text{CySalenSO}_3)_2\text{Cu}$ (3) (green) ($\mu_0 H = 0.5$ T).

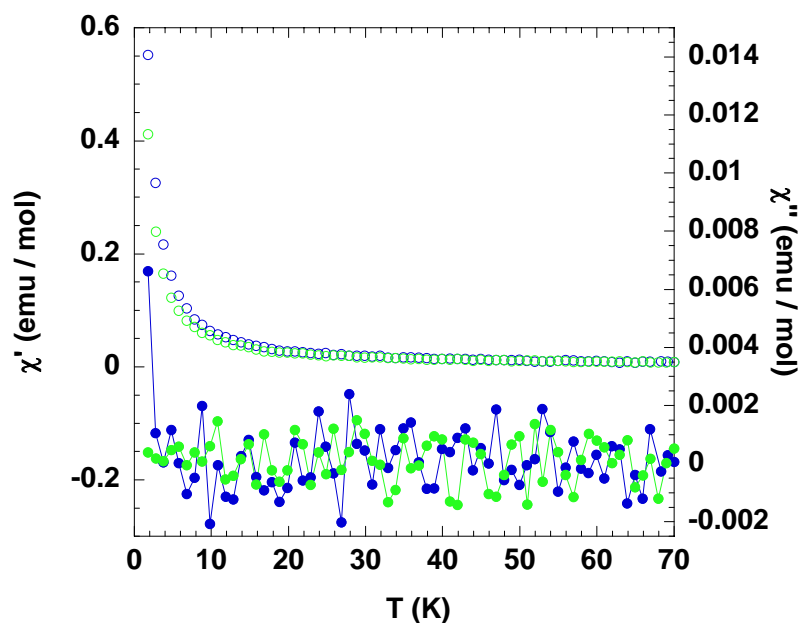


Fig. S9 In-phase (open circles) and out-of-phase (filled circles, full line is just a guide for the eyes) susceptibility (χ' and χ'' respectively) for **Ni(SalenSO₃)Cu (1)** (blue) and **Ni((R,R)CySalenSO₃)Cu (3)** (green) ($\mu_0 H_{ac} = 0.35$ mT, $f = 100$ Hz).

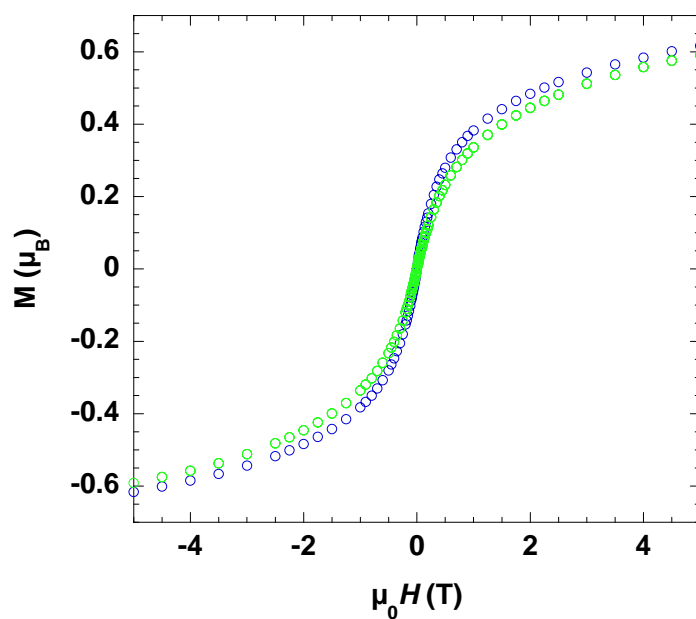


Fig. S10 $M = f(H)$ for **Ni(SalenSO₃)Cu (1)** (blue) and **Ni((R,R)CySalenSO₃)Cu (3)** (green) ($T = 1.8$ K).

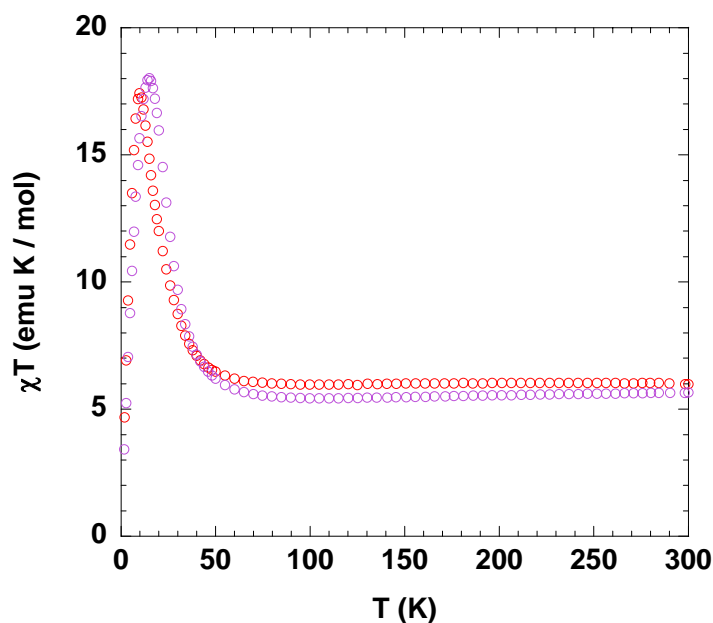


Fig. S11 $\chi T = f(T)$ for $\text{Ni}(\text{SalenSO}_3)_2\text{Co}$ (2) (red) and $\text{Ni}((R,R)\text{CySalenSO}_3)_2\text{Co}$ (5) (purple) ($\mu_0 H = 0.5$ T).

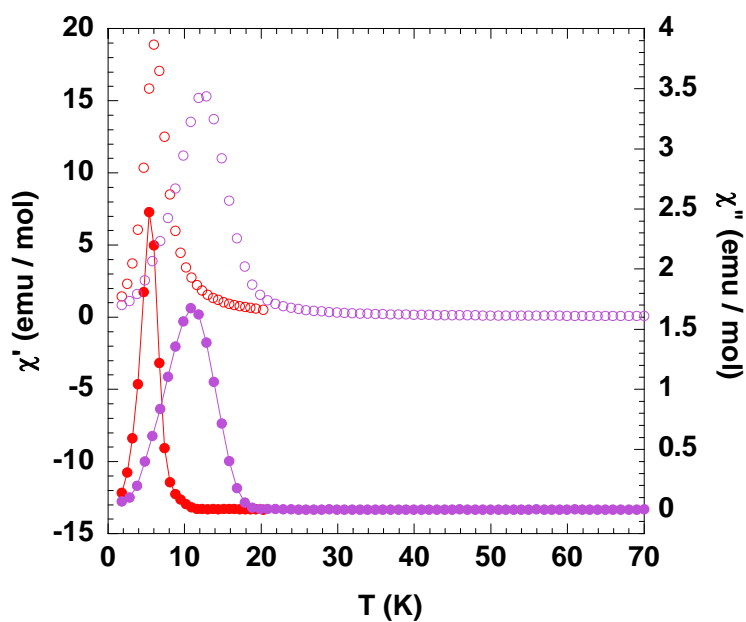


Fig. S12 In-phase (open circles) and out-of-phase (filled circles, full line is just a guide for the eyes) susceptibility (χ' and χ'' respectively) for $\text{Ni}(\text{SalenSO}_3)_2\text{Co}$ (2) (red) and $\text{Ni}((R,R)\text{CySalenSO}_3)_2\text{Co}$ (5) (purple) ($\mu_0 H_{ac} = 0.35$ mT, $f = 100$ Hz).

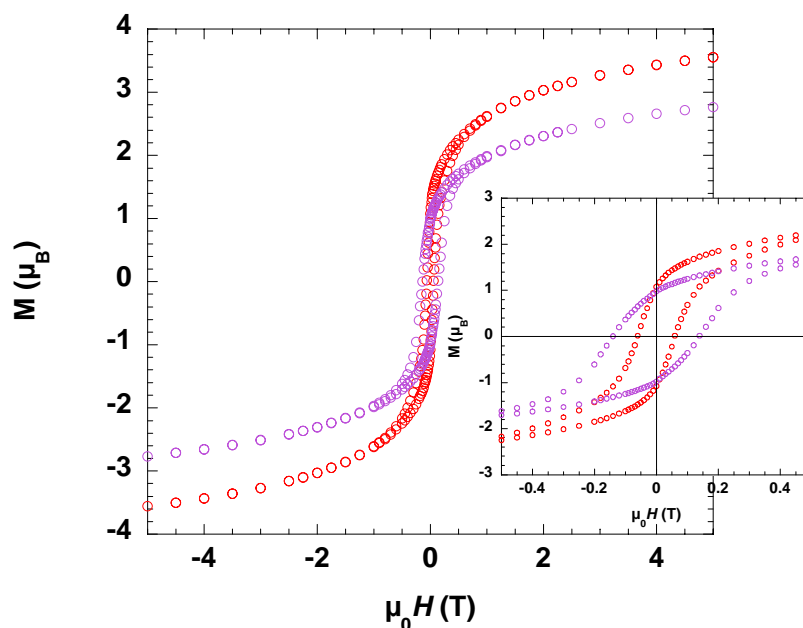


Fig. S13 $M = f(H)$ for $\text{Ni}(\text{SalenSO}_3)_2\text{Co}$ (**2**) (red) and $\text{Ni}((\text{R,R})\text{CySalenSO}_3)_2\text{Co}$ (**5**) (purple) ($T = 1.8$ K).

- 1 E. Delahaye, M. Diop, R. Welter, M. Boero, C. Massobrio, P. Rabu and G. Rogez, *Eur. J. Inorg. Chem.*, in press.
- 2 V. Laget, C. Hornick, P. Rabu and M. Drillon, *J. Mater. Chem.*, 1999, **9**, 169-174.
- 3 V. Laget, Ph.D thesis, Strasbourg, 1998.
- 4 N. Masciocchi, E. Corradi, A. Sironi, G. Moretti, G. Minelli and P. Porta, *J. Sol. St. Chem.*, 1997, **131**, 252-262.
- 5 P. Rabu, S. Angelov, P. Legoll, M. Belaiche and M. Drillon, *Inorg. Chem.*, 1993, **32**, 2463-2468.
- 6 A. Demessence, G. Rogez and P. Rabu, *Chem. Mater.*, 2006, **18**, 3005-3015.
- 7 L. Poul, N. Jouini and F. Fievet, *Chem. Mater.*, 2000, **12**, 3123-3132.
- 8 C. O. Oriakhi, I. V. Farr and M. M. Lerner, *J. Mater. Chem.*, 1996, **6**, 103-107.
- 9 M. Taibi, S. Ammar, N. Jouini, F. Fiévet, P. Molinié and M. Drillon, *J. Mater. Chem.*, 2002, **12**, 3228-3244.
- 10 S. Pillet, M. Souhassou, C. Lecomte, P. Rabu, M. Drillon and C. Massobrio, *Phys Rev. B*, 2006, **73**, 115116.
- 11 S.-H. Park and C. E. Lee, *J. Phys. Chem. B*, 2005, **109**, 1118-1124.
- 12 V. Laget, C. Hornick, P. Rabu, M. Drillon and R. Ziessel, *Coord. Chem. Rev.*, 1998, **178-180**, 1533-1553.
- 13 K. Nakamoto, *Infrared and Raman Spectra of Inorganic and Coordination Compounds, Fourth Edition*, Wiley Interscience, New York, 1986.
- 14 C. Bauer, P. Jacques and A. Kalt, *Chem. Phys. Lett.*, 1999, **307**, 397-406.
- 15 M. Kurmoo, P. Day, A. Derory, C. Estournès, R. Poinso, M. J. Stead and C. J. Kepert, *J. Sol. St. Chem.*, 1999, **145**, 452-459.